error floor as SNR increases. The CRB is derived, and the numeral results are provided which corroborate the proposed studies.

REFERENCES

[1] Y. Yao and G. B. Giannakis, "Blind carrier frequency offset estimation in SISO, MIMO, and multiuser OFDM systems," *IEEE Trans. Commun.*, vol. 53, no. 1, pp. 173–183, Jan. 2005.

[2] T. Roman, S. Visuri, and V. Koivunen, "Blind frequency synchronization in OFDM via diagonality criterion," *IEEE Trans. Signal Process.*, vol. 54, no. 8, pp. 3125–3135, Aug. 2006.

[3] B. Chen and H. Wang, "Blind estimation of OFDM carrier freuqnecy offset via oversampling," *IEEE Trans. Signal Process.*, vol. 52, no. 7, pp. 2047–2057, Jul. 2004.

[4] H. G. Jeon, K. S. Kim, and E. Serpedin, "An efficient blind deterministic frequency offset estimation for OFDM systems," *IEEE Trans. Commun.*, vol. 59, no. 4, pp. 1133–1141, Apr. 2011.

[5] H. Liu and U. Tureli, "A high-efficiency carrier estimator for OFDM communications," *IEEE Commun. Lett.*, vol. 2, no. 4, pp. 104–106, Apr. 1998.

[6] B. Chen, "Maximum likelihood estimation of OFDM carrier frequency offset," *IEEE Signal Process. Lett.*, vol. 9, no. 4, pp. 123–126, Apr. 2002.

[7] W. Zhang and Q. Yin, "Blind maximum likelihood carrier frequency offset estimation for OFDM with multi-antenna receiver," *IEEE Trans. Signal Process*, vol. 61, no. 9, pp. 2295–2307, May 2013.

[8] W. Zhang, Q. Yin, W. Wang, and F. Gao, "One-shot blind CFO and channel estimation for OFDM with multi-antenna Receiver," *IEEE Trans. Signal Process.*, vol. 62, no. 15, pp. 3799–3808, Aug. 2014.

[9] W. Zhang, Q. Yin, and W. Wang, "Blind closed-form carrier frequency offset estimation for OFDM with multi-antenna receiver," *IEEE Trans. Veh. Technol.*, vol. 64, no. 8, pp. 3850–3856, Aug. 2015.

[10] T. Roman and V. Koivunen, "One-shot subspace based method for blind CFO estimation for OFDM," in *Proc. ICASSP*, 2005, pp. iii/809–iii/812.

[11] T. Roman and V. Koivunen, "Subspace method for blind CFO estimation for OFDM systems with constant modulus constellations," in *Proc. IEEE VTC Spring*, 2005, vol. 2, pp. 1253–1257.

[12] J. Oh, J. Kim, and J. Lim, "Blind carrier frequency offset estimation for OFDM systems with constant modulus constellations," *IEEE Commun. Lett.*, vol. 15, no. 9, pp.971–973, Sep. 2011.

[13] S. Lmai, A. Bourre, C. Laot, and S. Houcke, "An efficent blind estimation of carrier frequency offset in OFDM systems," *IEEE Trans. Veh. Technol.*, vol. 63, no. 4, pp. 1945–1950, May 2014.

[14] Z. Xiang and A. Ghrayeb, "A blind carrier frequency offset estimation scheme for OFDM systems with constant modulus signaling," *IEEE Trans. Commun.*, vol. 56, no. 7, pp. 1032–1037, Jul. 2008.

[15] S. Younis, B. Sharif, C. Tisimendis, A. Dweik, and A. Hazmi, "Blind scheme for carrier frequency offset estimation in MIMO-OFDM systems," in *Proc. IEEE ISSPIT*, 2009, pp. 1–4.

[16] L. Wu, X. Zhang, and P. Li, "A low-complexity blind carrier frequency offset estimator for MIMO-OFDM systems," *IEEE Signal Process. Lett.*, vol. 15, pp. 769–772, 2008.

[17] J. Chen, Y.-C. Wu, S. Ma, and T.-S. Ng, "Joint CFO and channel estimation for multiuser MIMO-OFDM systems with optimal traning sequences," *IEEE Trans. Signal Process.*, vol. 56, no. 8, pp. 4008–4019, Aug. 2008.

[18] P. Stoica and A. Nehorai, "Performance study of conditional and unconditional direction-of-arrival estimation," *IEEE Trans. Acoust., Speech, Signal Process.*, vol. 38, no. 10, pp. 1783–1795, Oct. 1990.

[19] P. Stoica and A. Nehorai, "MUSIC, maximum likelihood, and Cramer-Rao blund," *IEEE Trans. Acoust., Speech, Signal Process.*, vol. 37, no. 5, pp. 720–741, May 1989.

[20] Y. R. Zheng and C. Xiao, "Simulation models with correct statistical properties for Rayleigh fading channels," *IEEE Trans. Commun.*, vol. 51, no. 6, pp. 920–928, Jun. 2003.

Location-Aware Pilot Assignment for Massive MIMO Systems in Heterogeneous Networks

Peiyao Zhao, Zhaocheng Wang, *Senior Member, IEEE*, Chen Qian, Linglong Dai, *Senior Member, IEEE*, and Sheng Chen, *Fellow, IEEE*

***Abstract*—We investigate the heterogeneous cellular network (HetNet) where the macrocell base stations (MBSs) are equipped with very large antenna arrays. Since such a combined massive multi-input multi-output (MIMO) and HetNet system operates in the co-channel time-division duplex mode, to mitigate the pilot contamination effect to channel estimation, the number of users that can be served simultaneously is limited by the available pilot resources in the conventional designs. We propose a pilot reuse scheme for massive MIMO–HetNet to increase the user capacity. Specifically, location-aware channel estimation is employed at the MBSs to mitigate the severe pilot contamination introduced by pilot reuse, and we propose a novel pilot assignment algorithm to reduce the interference in HetNets. Simulation results demonstrate that our proposed scheme can support more users and increase both the uplink and the downlink sum-rate capacity, in comparison to the conventional scheme, particularly when the antenna number at the MBSs is sufficiently large.**

***Index Terms*—Heterogeneous network (HetNet), location-aware pilot assignment, massive multi-input multi-output (MIMO), pilot contamination.**

I. INTRODUCTION

Massive multi-input multi-output (MIMO) and heterogeneous cellular network (HetNet) are regarded as two promising techniques to meet the huge capacity needs for wireless communications. A massive MIMO system, in which the number of antennas employed at each cell cite is large, exploits the spatial degrees of freedom to serve several users on the same time/frequency resource [1], [2]. It has been proved in [3] that for massive MIMO systems, high spectral and energy efficiency can be achieved by using simple linear signal processing algorithms. A HetNet, on the other hand, exploits spatial reuse gains through the deployment of small cells [4], in which the distance between the small-cell users (SUs) and their associated small-cell base stations (SBSs) is significantly reduced, so that local capacity enhancements are provided. A combined massive MIMO and HetNet system consists of two tiers [5], namely, the primary tier, which includes several macrocell base stations (MBSs) with very large

Manuscript received April 30, 2015; revised August 20, 2015 and September 11, 2015; accepted September 18, 2015. Date of publication September 22, 2015; date of current version August 11, 2016. This work was supported in part by the National Natural Science Foundation of China under Grant 61271266, by the National Key Basic Research Program of China under Grant 2013CB329203, by the National High Technology Research and Development Program of China under Grant 2014AA01A704, by Beijing Natural Science Foundation under Grant 4142027, and by the Foundation of Shenzhen Government. The review of this paper was coordinated by Prof. R. Dinis.

P. Zhao, Z. Wang, C. Qian, and L. Dai are with the Tsinghua National Laboratory for Information Science and Technology, Department of Electronic Engineering, Tsinghua University, Beijing 100084, China (e-mail: pdszpy19930218@163.com; zcwang@tsinghua.edu.cn; qc8802@gmail.com; daill@tsinghua.edu.cn).

S. Chen is with the School of Electronics and Computer Science, University of Southampton, Southampton SO17 1BJ, U.K., and also with King Abdulaziz University, Jeddah 21589, Saudi Arabia (e-mail: sqc@ecs.soton.ac.uk).

Color versions of one or more of the figures in this paper are available online at http://ieeexplore.ieee.org.

Digital Object Identifier 10.1109/TVT.2015.2480965

0018-9545 © 2015 IEEE. Personal use is permitted, but republication/redistribution requires IEEE permission.
See http://www.ieee.org/publications_standards/publications/rights/index.html for more information.

antenna arrays, and the secondary tier of SBSs, each equipped with a single antenna.

It is well known that the time-division duplex (TDD) protocol utilizing the channel reciprocity reduces the overhead of training for the massive MIMO scenario. Thus, we assume that the envisaged massive MIMO–HetNet system operates in a co-channel TDD (coTDD) mode [6], in which the uplink and downlink transmissions are synchronized in both tiers. As demonstrated in [7], the pilot contamination effect, which is caused by utilizing non-orthogonal pilot sequences in adjacent cells, limits the capacity of the system. In the previous work [8], orthogonal pilots are assigned to the macrocell users (MUs) and SUs inside the same macrocell to prevent severe interference in the uplink training stage, which is referred to as the conventional scheme in this paper. With this conventional design, the number of users that can be served simultaneously is small, and the sum-rate capacity of the system is limited.

Many solutions have been proposed to reduce the pilot contamination effect [7], [9], [10], among which the location-aware channel estimation [10] introduces a fast Fourier transform (FFT)-based postprocessing after the conventional pilot-aided channel estimation to efficiently eliminate the interference from the users with different angle of arrivals (AOAs) at the base station (BS). We notice that the positions of SUs are restricted in a small region around the corresponding SBSs in HetNets, which leads to the relatively stable AOAs at the MBSs. Thus, it is possible to employ the location-aware channel estimation at the MBSs. However, it should be noticed that the pilot assignment algorithm proposed in [10] was originally designed to reduce the intercell interference (ICI) in homogeneous networks, but it is not suitable for the HetNet scenario since the intertier interference is not modeled and considered in [10]. The idea of utilizing AoAs to distinguish different users was also proposed in [11] and [12], in which the cell sectorization-base pilot assignment algorithm is applied. However, the schemes proposed in these two works were originally designed to reduce the ICI in homogeneous networks [11] or in single-cell cases [12], but they are not suitable for our HetNet scenario.

In this paper, we propose a pilot reuse scheme for the HetNet scenario to support more users. More specifically, the location-aware channel estimation is employed at the MBSs to mitigate the severe pilot contamination introduced by pilot reuse, and our other main contribution includes developing a novel pilot assignment algorithm to reduce the interference in HetNets, which guarantees that the users with the same pilot have distinguishable AOAs at the MBSs, whereas the distances between the interfering users and the corresponding SBSs are sufficiently large. Simulation results show that our proposed scheme can support more users and increase the sum-rate capacity of the system significantly. Moreover, little coordination between BSs is required in our scheme, which leads to low implementation complexity.

II. Background

Consider a HetNet with L macrocells, each consisting of P overlaid small cells, as shown in Fig. 1. We assume that K_m single-antenna MUs are served at the same time/frequency resource in each macrocell, and only one SU with a single antenna is supported in each small cell. The MBSs are equipped with M antennas with $M \gg K_m$, whereas the SBSs only have a single antenna [6]. Furthermore, we define all the users, including MUs and SUs, inside the same macrocell as a user group. The system operates in coTDD mode to prevent large overhead of training.

A. System Signal Model

At the uplink training stage, all users from all cells transmit the pilot signals to their corresponding BSs [8]. Denote the column vector

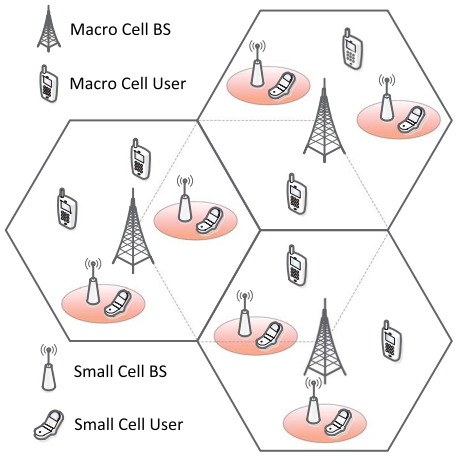

Fig. 1. Illustrative example of a heterogeneous network comprising $L = 3$ macrocells each with $P = 2$ small cells.

$\boldsymbol{\phi}_k = [\phi_{k,1}\phi_{k,2}, \ldots, \phi_{k,\tau}]^T \in \mathbb{C}^{\tau\times 1}$ as the pilot sequence with length τ adopted by the kth MU in each user group, where $1 \le k \le K_m$ and $\boldsymbol{\phi}_k^T\boldsymbol{\phi}_k^* = 1$, whereas $()^T$ and $()^*$ denote the transpose and conjugate operators, respectively. The pilot sequences $\boldsymbol{\phi}_k$ for $1 \le k \le K_m$ are orthogonal, i.e., $\boldsymbol{\phi}_i^T\boldsymbol{\phi}_j^* = 0$ for $i \ne j$, and they are shared by all the user groups. To save the limited pilot resources, the SUs in each user group reuse part of the pilot sequences, which is denoted by $\boldsymbol{\phi}'_k = \boldsymbol{\phi}_{s_k} \in \{\boldsymbol{\phi}_1, \boldsymbol{\phi}_2, \ldots, \boldsymbol{\phi}_{K_m}\}$, $1 \le k \le P$, where $\boldsymbol{\phi}'_k$ is the pilot sequence adopted by the kth SU. That is, the kth SU reuses the pilot sequence of the s_kth MU in the same user group, where $s_k \in \{1, 2, \ldots, K_m\}$. Note that, in practice, the number of overlaid small cells is no more than the number of supported MUs, i.e., $P \le K_m$.

At the lth MBS, the received signal matrix $\boldsymbol{Y}_l \in \mathbb{C}^{M\times\tau}$ can be expressed as

$$\boldsymbol{Y}_l = \sum_{j=1}^{L}\sum_{k=1}^{K_m} \boldsymbol{h}_{l,j,k}\boldsymbol{\phi}_k^T + \sum_{j=1}^{L}\sum_{k=1}^{P} \boldsymbol{h}'_{l,j,k}\boldsymbol{\phi}_{s_k}^T + \boldsymbol{N}_l \tag{1}$$

where $\boldsymbol{N}_l \in \mathbb{C}^{M\times\tau}$ is the additive white Gaussian noise (AWGN) matrix, whereas $\boldsymbol{h}_{l,j,k_m} \in \mathbb{C}^{M\times 1}$ and $\boldsymbol{h}'_{l,j,k_s} \in \mathbb{C}^{M\times 1}$ denote the channel vectors linking the k_mth MU and the k_sth SU in the jth user group to the lth MBS, respectively. Right multiplying $\boldsymbol{Y}_l$ by $\boldsymbol{\phi}_k^*$ yields the least squares (LS) channel estimation [7] of the kth MU as

$$\widehat{\boldsymbol{h}}_{l,l,k} = \boldsymbol{h}_{l,l,k} + \underbrace{\sum_{j=1,j\ne l}^{L} \boldsymbol{h}_{l,j,k}}_{\substack{\text{intercell}\\ \text{interference}}} + \underbrace{\sum_{j=1}^{L}\sum_{s_i=k} \boldsymbol{h}'_{l,j,i}}_{\substack{\text{intertier}\\ \text{interference}}} + \boldsymbol{n}_{l,k} \tag{2}$$

where $\boldsymbol{n}_{l,k} = \boldsymbol{N}_l\boldsymbol{\phi}_k^*$ is the equivalent noise vector. It can be seen that the interference comprises the intercell part, which is introduced by the MUs in the adjacent user groups, and the intertier part, which comes from the SUs adopting the same pilot sequence.

Let g_{l,i,j,k_m} and g'_{l,i,j,k_s} be the channel coefficients linking the k_mth MU and the k_sth SU in the jth user group to the ith SBS in the lth macrocell, respectively. Then, the received signal vector $\boldsymbol{y}'_{l,i} \in \mathcal{C}^{\tau\times 1}$ at the ith SBS in the lth macrocell is given as

$$\boldsymbol{y}'_{l,i} = \sum_{j=1}^{L}\sum_{k=1}^{K_m} g_{l,i,j,k}\boldsymbol{\phi}_k + \sum_{j=1}^{L}\sum_{k=1}^{P} g'_{l,i,j,k}\boldsymbol{\phi}_{s_k} + \boldsymbol{\xi}_{l,i} \tag{3}$$

where $\boldsymbol{\xi}_{l,i}$ is the corresponding AWGN vector. Left multiplying $\boldsymbol{y}'_{l,i}$ by $\boldsymbol{\phi}_{s_i}^H$ obtains the LS channel estimation of the link between the ith SU and its corresponding SBS in the lth user group as

$$\widehat{g}'_{l,i,l,i} = g'_{l,i,l,i} + \underbrace{\sum_{j=1}^{L} g_{l,i,j,s_i}}_{\substack{\text{intertier}\\ \text{interference}}} + \underbrace{\sum_{s_k=s_i,k\neq i} g'_{l,i,l,k} + \sum_{j=1,j\neq l}^{L}\sum_{s_k=s_i} g'_{l,i,j,k}}_{\substack{\text{intercell}\\ \text{interference}}} + \varepsilon_{l,i} \quad (4)$$

where $\varepsilon_{l,i} = \boldsymbol{\phi}_{s_i}^H \boldsymbol{\xi}_{l,i}$ is the equivalent noise, and $()^H$ is the Hermitian transpose operator. It can be seen that the intertier interference comes from the s_ith MU of each user group, and the ICI is caused by other SUs with the same pilot. Furthermore, the first part of the ICI comes from the SUs in the same user group, and the second part comes from the SUs in the adjacent user groups.

We adopt the narrow-band channel model given in [13]. Then, the channel coefficient vector $\boldsymbol{h}_{l,j,k} \in \mathbb{C}^{M\times 1}$, for example, takes the following expression:

$$\boldsymbol{h}_{l,j,k} = \frac{1}{\sqrt{Q}} \sum_{q=1}^{Q} \beta_{l,j,k}^{(q)} \boldsymbol{\alpha}\left(\theta_{l,j,k}^{(q)}\right) \quad (5)$$

where Q is the number of the paths between the kth MU in the jth user group to the lth MBS, $\beta_{l,j,k}^{(q)}$ is the large-scale fading coefficient of the qth path between the kth MU in the jth user group to the lth MBS, and $\theta_{l,j,k}^{(q)}$ is the AOA of this qth path, whereas $\boldsymbol{\alpha}(\theta) \in \mathbb{C}^{M\times 1}$ denotes the steering vector with AOA θ. For uniformly spaced linear array, the steering vector $\boldsymbol{\alpha}(\theta)$ takes the following expression:

$$\boldsymbol{\alpha}(\theta) = \left[e^{\mathrm{j}\Phi} e^{\mathrm{j}\left(2\pi \frac{D}{\lambda} \sin\,\theta + \Phi\right)}, \ldots, e^{\mathrm{j}\left(2\pi \frac{(M-1)D}{\lambda} \sin\,\theta + \Phi\right)}\right]^T \quad (6)$$

where λ is the wavelength, $D \leq \lambda/2$ is the antenna spacing at BSs, and Φ is a random phase, whereas $\mathrm{j} = \sqrt{-1}$. For the channel coefficient vector $\boldsymbol{h}'_{l,j,k} \in \mathbb{C}^{M\times 1}$, we have a similar expression. Note that the variance of angle spread is generally small in the scenario of macrocell [13], which means that the AOAs of most signal components fall in an interval $[\theta_{\min}, \theta_{\max}]$.

B. Location-Aware Channel Estimation

The location-aware channel estimation scheme of [10] introduces postprocessing after the conventional pilot-aided channel estimation to reduce the interference from the users with different AOAs significantly. This location-aware channel estimation requires the condition of distinguishable AOAs between the desired signal and the interference, and its performance is strongly dependent on the length of the channel vector, i.e., the number of antennas employed at BSs. Therefore, this scheme is only suitable for MBSs, for the reason that the angle spread in the scenario of the macrocell can be small and the MBSs are equipped with a large number of antennas.

By dropping the subscripts in the estimated channel vector (2), it is simplified to

$$\widehat{\boldsymbol{h}} = \boldsymbol{h} + \boldsymbol{h}^{(I)} + \boldsymbol{n} \quad (7)$$

where $\boldsymbol{h}$ is the desired channel vector, and $\boldsymbol{h}^{(I)}$ represents the aggregate of all the interfering channels. We assume that the AOAs of $\boldsymbol{h}$ are limited in $[\theta_{\min}, \theta_{\max}]$, which is justified in [13]. Denote the N-point FFTs of $\widehat{\boldsymbol{h}}$ and $\boldsymbol{h}$ by $\widehat{\boldsymbol{F}}$ and $\boldsymbol{F}$, respectively. The steering vector given in (6) can be regarded as a single-frequency signal with frequency $f_\alpha = (D/\lambda)\sin(\theta)$ when the antenna number M is sufficiently large, and its FFT tends to be a δ-function at $\lfloor g_N(\theta) \rceil$, where

$$g_N(\theta) = \begin{cases} N - N\frac{D}{\lambda}\sin(\theta), & \theta \in \left[-\frac{\pi}{2}, 0\right) \\ N\frac{D}{\lambda}\sin(\theta), & \theta \in \left[0, \frac{\pi}{2}\right) \end{cases} \quad (8)$$

and $\lfloor\cdot\rceil$ denotes the integer rounding operator. Therefore, most energy of $\boldsymbol{F}$ falls in the interval $I(k_{\min}, k_{\max})$, where

$$I(k_{\min}, k_{\max}) = \begin{cases} [0, k_{\max}] \cup [k_{\min}, N], & \text{for } -\pi/2 \leq \theta_{\min} < 0 \\ & \quad < \theta_{\max} \leq \pi/2 \\ [k_{\min}, k_{\max}], & \text{otherwise} \end{cases} \quad (9)$$

whereas $k_{\min} = \lfloor g_N(\theta_{\min}) \rceil$ and $k_{\max} = \lfloor g_N(\theta_{\max}) \rceil$. By forcing the value of $\widehat{\boldsymbol{F}}$ outside the interval $I(k_{\min}, k_{\max})$ to zero, the interference with different AOAs is reduced, whereas the effect of the noise is also mitigated. Consequently, we obtain a more accurate estimation $\widetilde{\boldsymbol{F}}$. Then, perform an inverse FFT operation on $\widetilde{\boldsymbol{F}}$ to get $\widetilde{\boldsymbol{f}} = [\widetilde{f}_0\ \widetilde{f}_1, \ldots, \widetilde{f}_{N-1}]^T$. Finally, the estimation of the channel coefficient vector is obtained as $\widetilde{\boldsymbol{h}} = [\widetilde{f}_0\ \widetilde{f}_1, \ldots, \widetilde{f}_{M-1}]^T$.

III. Location-Aware Pilot Assignment

In the conventional scheme, the pilot sequences adopted by the MUs and SUs inside the same user group are orthogonal to prevent the severe intertier interference. Hence, the number of users that can be served simultaneously is limited to $K_m + P \leq \tau$, and the achievable sum rate of the system is thus limited. To overcome this drawback, we propose a location-aware pilot assignment scheme for HetNets in which the location-aware channel estimation is employed at the MBSs, and the SUs reuse part of the orthogonal pilot sequences to support more users with the limited pilot resources. The interference in HetNets is reduced with an elaborate pilot assignment pattern, which enhances the achievable sum rate of the system.

Consider first the interference from the jth interfering user to the kth MU in the lth macrocell. Denote $\theta_{j,l}$ and $\theta_{k,l}$ as the AOAs of the interfering user and the desired MU at the lth MBS, respectively, and $d_{j,l}$ as the distance between the interfering user and the lth MBS. We use the metric of [10] to measure the interference at the MBS, which is given by

$$R_{j,l,k} = \frac{\boldsymbol{t}^T(\theta_{j,l})\boldsymbol{t}(\theta_{k,l})}{d_{j,l}^{\gamma}} \quad (10)$$

where $\boldsymbol{t}(\theta) = [\cos\,\theta\ \ \sin\,\theta]^T$ is the directional vector, and γ is the path-loss exponent. The interfering user may be an MU or an SU, which corresponds to the ICI and intertier interference, respectively. Thus, the interference to all the MUs can be summed up by

$$I_m = \sum_{l=1}^{L}\sum_{k=1}^{K_m}\sum_{j=1,j\neq l}^{L} R_{j,l,k} + \sum_{l=1}^{L}\sum_{k=1}^{K_m}\sum_{s_i=k} R_{i,l,k}. \quad (11)$$

However, the location-aware pilot assignment proposed in [10] cannot be applied to the SBSs, as every SBS only equips with a single antenna. To develop a pilot assignment scheme that is applicable to HetNets, we propose to measure the interference from the jth interfering user to the kth desired SU in the lth user group by the following metric:

$$R'_{j,l,k} = \frac{1}{d_{j,l,k}^{\gamma}} \quad (12)$$

where $d_{j,l,k}$ is the distance between the jth interfering user and the considered kth SBS in the lth macrocell. Again, the interfering user can be an MU or an SU, corresponding to the intertier interference and ICI, respectively. The interference to all the SUs can be summed up by

$$I_s = \sum_{l=1}^{L}\sum_{k=1}^{P}\sum_{j=1}^{L} R'_{j,l,k} + \sum_{l=1}^{L}\sum_{k=1}^{P}\sum_{s_i=s_k, i\neq k} R'_{i,l,k} \tag{13}$$

where the summation range $s_i = s_k, i \neq k$ indicates the SUs that adopt the same pilot, excluding the considered SU itself.

Finally, the criterion that measures the interference in HetNets can be defined by

$$I = I_m + \alpha I_s \tag{14}$$

where α is a weighting value to balance the interference to MUs and SUs. Since we treat MUs and SUs equally, we apply the equal weighting of $\alpha = 1$. The optimal pilot assignment scheme should arrange the pilots online to minimize I of (14) according to the locations of users served. However, it is impractical to implement due to prohibitively high complexity and the needs for collaboration between BSs. In particular, finding the optimal pilot assignment pattern by an exhaustive search requires examining a total of $(K_m!K_m^P)^L$ pilot assignment patterns, which is impossible to do for massive MIMO–HetNet. Therefore, we propose an efficient algorithm to obtain a suboptimal pilot assignment pattern.

When a MIMO–HetNet is deployed, the number of MUs supported per macrocell K_m is fixed, but the locations of MUs are random, and MUs are mobile with the channel coherent time related to the mobility of MUs, whereas the number of small cells within each macrocell P is also known, and the locations of small cells are also random, but they are fixed. Hence, our novel pilot assignment procedure consists of a four-step algorithm and an adjustment algorithm.

A. Four-Step Algorithm

At the MIMO–HetNet deployment stage, we divide each hexagonal macrocell into $S = K_m$ sectors uniformly and preassign the pilot of each sector, as well as each small cell. That is, the MBS selects one user from each sector to serve at the same time/frequency resource, i.e., we initially assume that each sector contains an MU, but later, we will modify the initial assignment to remove this assumption. We also assume that all the SUs locate at the centers of their small cells, which is reasonable considering the small size of small cells.

Due to the large path loss, the interference attenuates quickly with the increase of the distance between an interfering user and the corresponding BS. Therefore, only the interference from the same and adjacent user groups, which is far larger than that from the other remote user groups, needs to be considered. Furthermore, the ICI to SUs can be reduced by minimizing the number of overlapping pilots reused in adjacent user groups. Note that if we have three distinct orthogonal pilot groups for small cells, the SUs in the adjacent user groups will not interfere with each other. In other words, the ICI to SUs can be completely eliminated. For example, consider the generic macrocell structure given in Fig. 2. Assume that each macrocell has two small cells, and we have the three distinct orthogonal pilot groups labeled $\{1, 2\}$, $\{3, 4\}$, and $\{5, 6\}$. By the pilot assignment for small cells, as shown in Fig. 2, the ICI from small cells located in adjacent macrocells can be completely removed. Let us define the pilot reuse factor of SUs as $p_{\text{reuse}} = (P/\tau)$. Then, if $p_{\text{reuse}} \leq (1/3)$, there exist three distinct sets of pilots, and the ICI between SUs is completely eliminated. However, if $p_{\text{reuse}} > (1/3)$, the ICI between SUs exists. In this case, we may first "omit" the ICI between SUs and search for the "optimal" pilot assignment pattern. Afterward, we check to see if there exists severe interference between SUs and adjust some pilots accordingly to avoid it. We now summarize the proposed four-step algorithm.

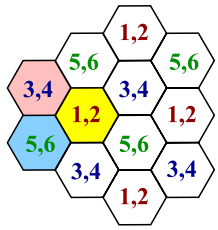

Fig. 2. Illustration of how to eliminate the ICI from the small cells located in other macrocells by the three distinct orthogonal pilot groups for small cells, where each macrocell has two small cells, and the three distinct orthogonal pilot groups are labeled $\{1, 2\}$, $\{3, 4\}$, and $\{5, 6\}$.

First Step: The sectors in the central macrocell are assigned with orthogonal pilots randomly. For each sector that has been assigned with pilot, check all the sectors in its nearest two adjacent macrocells by calculating the corresponding interference metrics and assign the sector that has the minimum interference with the same pilot. After all possible sectors are assigned, there may still remain some unassigned sectors.

Second Step: We assign the pilots of SUs in the central user group. After the first step, we have obtained an incomplete pilot assignment for macrocells, based on which we calculate the intertier interference to the SUs in the central group under different pilot reuse patterns and assign these SUs with the pattern of minimum intertier interference. Then, we determine the set of pilots adopted by the SUs in each adjacent user group by minimizing the number of overlapping pilots. In this step, only the pilots of SUs in the central group are actually assigned. For other user groups, the sets of SU pilots are determined but are not assigned to each SU yet.

Third Step: The remaining unassigned sectors and SUs are assigned with pilots by exhaustive search to achieve the smallest interference metric I. To further reduce the complexity, when calculating the intertier interference to MUs, we only consider the SUs inside the same user group, as this kind of intertier interference, due to the small distance, is generally far stronger than that from the SUs in other user groups. Normally, the number of unassigned sectors left in each macrocell is small, and the set of SU pilots for each user group has been already determined. Thus, the complexity of exhaustive search in this step is acceptable.

Fourth Step: We reconsider the ICI between SUs if the pilot reuse factor of SUs $p_{\text{reuse}} > 1/3$. We check the ICI between the SUs assigned with the same pilot. If there exists some severe interference, we go back to the third step and find a better solution under the condition that the considered SUs with severe interference use different pilots.

This algorithm is capable of finding a suboptimal pilot assignment with acceptable computational complexity. The exact complexity is difficult to quantify, as it is related to the specific topology of the MIMO–HetNet under consideration. However, its complexity is much lower than that of the exhaustive search, which requires examining all the $(K_m!K_m^P)^L$ pilot assignment patterns. It should be noted that the algorithm is performed only once based on the deployment of the MIMO–HetNet system, and the obtained pilots are assigned to each sector and each small cell. Moreover, the channel coherence time does not affect this four-step algorithm, as the algorithm is independent of the actual location distribution of MUs.

B. Adjustment Algorithm

The assumption that each sector contains one and only one user is, of course, hard to guarantee in practice. In the situation that there exist a few sections each containing more than one user, while some other sectors are blank, we need to modify the pilot assignment obtained by the above four-step algorithm. Specifically, one user is randomly selected from each sector that contains more than one user to adopt the pilot associated with the sector, whereas the remaining users have to be assigned with the pilots associated with the blank sectors. To reduce the complexity, we arrange the unadopted pilots to the unassigned MUs in each macrocell separately, which means that when we consider this pilot adjustment in one cell, all the other cells are assumed to be assigned with the pilot pattern obtained by the four-step algorithm. Let us consider this pilot reassignment for macrocell l with K_r^l as the number of the remaining unassigned MUs and $\{p_1^l, \ldots, p_{K_r^l}^l\}$ as the index set of the unadopted pilots in macrocell l, respectively, where $1 \le l \le L$. Similarly, we perform this task by minimizing the criterion

$$I_r^l = \sum_{k=1}^{K_r^l} \sum_{j=1, j\neq l}^{L} R_{j,l,p_k^l} + \sum_{k=1}^{K_r^l} \sum_{s_i = p_k^l} R_{i,l,p_k^l} \tag{15}$$

based on exhaustive search. It can be proved that the expectation of K_r^l, which is denoted by $E\{K_r^l\}$, is much smaller than K_m. Thus, the complexity of this exhaustive search for reassignment, which is given as $K_r^l!$, is acceptable. With this readjustment, our proposed location-aware pilot assignment scheme can be applied to any type of distribution for user locations.

Since the pilot assignment pattern obtained by the four-step algorithm is static, the setup or online time of the whole pilot assignment depends only on the pilot readjustment process. Therefore, the proposed pilot assignment algorithm is capable of converging within the channel coherence time due to the low complexity of this pilot readjustment process.

Given the same training overhead, our location-aware pilot assignment scheme increases the number of users supported. Moreover, the location-aware channel estimation is employed as the MBSs to eliminate the interference from the users with different AOAs. Consequently, the sum-rate capacity of both the uplink and downlink transmissions are increased significantly, as will be shown in the next section.

IV. Simulation Results

A massive MIMO–HetNet with $L = 7$ macrocells is simulated, and the users in the center cell, which is denoted by cell 0, are the target users, whereas the adjacent cells are the interference cells. The parameters of this simulated massive MIMO–HetNet are listed in Table I. For the conventional scheme, $K_m = \tau - P = 8$ MUs are supported simultaneously to guarantee the orthogonality of the pilots inside the same user group. The MUs and SUs randomly locate in the corresponding cells, and their pilots are randomly assigned as well. By contrast, our proposed location-aware pilot assignment scheme can support $K_m = \tau = 12$ MUs per macrocell simultaneously, as the $P = 4$ SUs in the same user group reuse part of the orthogonal pilots. The MUs and SUs of each cell are also randomly located. Furthermore, for our scheme, the location-aware channel estimation is carried out at MBSs, with the size of FFT fixed to $N = 8192$. The macrocell is divided into $S = \tau = 12$ sectors, and the four-step algorithm is applied to obtain a suboptimal pilot assignment pattern for each sector and each SU. A typical example of the obtained pilot assignment pattern for this MIMO–HetNet is shown in Fig. 3. As the locations of the MUs in each macrocell are actually random, the adjustment to the pilot assignment pattern obtained by the four-step algorithm is then carried out to complete the actual assignment of each pilot to an MU.

TABLE I
Parameters of the Simulation System

Macro cell radius	500 m
Path-loss exponent	3.5
Variance of shadow fading	8 dB
Carrier frequency	2 GHz
Antenna spacing D	$\lambda/2$
Standard deviation of angle spread	8 degree
Number of orthogonal pilots τ	12
Number of small-cells per macro-cell P	4
Transmit powers	MBS: 46 dBm
	SBS: 24 dBm
Signal-to-noise ratio (SNR)	MU: 20 dB
	SU: 30 dB

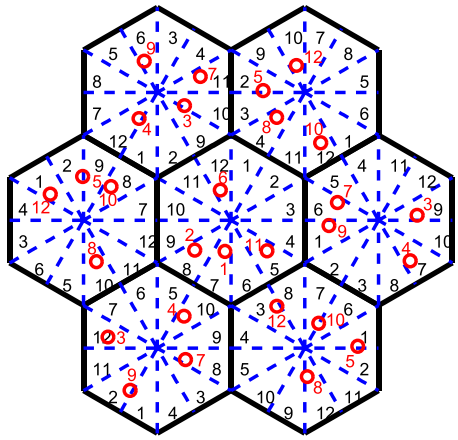

Fig. 3. Typical pilot assignment pattern obtained by the proposed four-step algorithm for randomly distributed SUs, where the red circle represents the small cell, and the black and red numbers denote the pilots assigned to the corresponding sector and small cell, respectively.

First, we investigate the per-user capacity of uplink data transmission. Matched-filter (MF) detection is applied at the MBSs. The capacities of MUs and SUs are obtained by averaging over the randomly located MUs and SUs in the central user group, respectively. The uplink capacity of the kth MU is calculated by [13]

$$C_{\mathrm{MU},k}^{\mathrm{uplink}} = \log_2\left(1 + \mathrm{SINR}_{\mathrm{MU},k}^{\mathrm{uplink}}\right) \tag{16}$$

with the uplink signal-to-noise-plus-interference ratio (SINR) of the considered MU denoted by $\mathrm{SINR}_{\mathrm{MU},k}^{\mathrm{uplink}}$. The definition of the uplink capacity of the kth SU, i.e., $C_{\mathrm{SU},k}^{\mathrm{uplink}}$, follows a similar expression. Fig. 4 shows the uplink per-user capacity as the function of the number of antennas employed at the MBS, where it can be seen that the uplink per-user capacity for SUs achieved by our scheme is smaller than that obtained by the conventional scheme. This is expected, as by increasing the number of the MUs supported to $K_m = \tau$, our scheme actually suffers from much severer interference due to the pilot reuse inside each user group. However, the proposed pilot assignment scheme is able to guarantee non-overlapping AOAs at the MBSs, which enables the location-aware channel estimation to reduce the pilot contamination effect. Consequently, the uplink per-user capacity for MUs achieved by our scheme remains nearly the same as the conventional scheme, which is confirmed by the results in Fig. 4. This, together with the fact that our scheme supports more Mus, ensures that

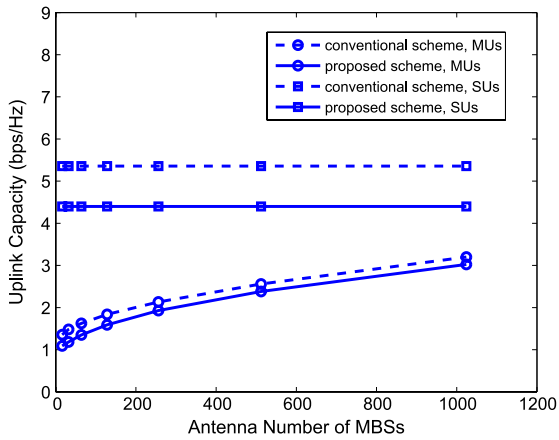

Fig. 4. Per-user capacity comparison of uplink data transmission with MF detection.

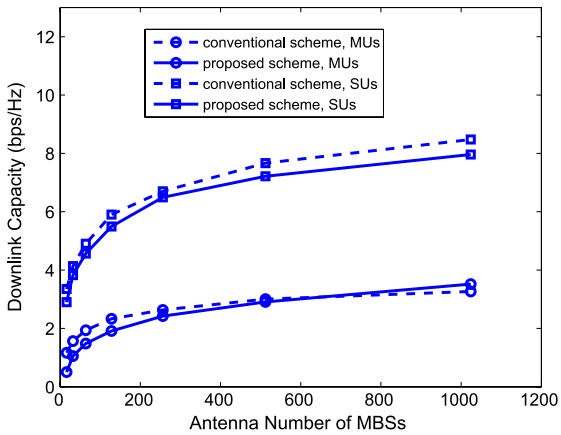

Fig. 5. Per-user capacity comparison of downlink data transmission with ZF precoding.

our scheme achieves a much higher sum rate or the total capacity per cell than the conventional one, which will be confirmed later.

Next, the per-user capacity of the downlink data transmission with zero-forcing (ZF) precoding is considered. The downlink capacity of the kth MU in the central group is defined as

$$C_{\mathrm{MU},k}^{\mathrm{downlink}} = \log_2\left(1 + \mathrm{SINR}_{\mathrm{MU},k}^{\mathrm{downlink}}\right) \tag{17}$$

where $\mathrm{SINR}_{\mathrm{MU},k}^{\mathrm{downlink}}$ is the SINR of the kth MU. The downlink capacity of the kth SU, i.e., $C_{\mathrm{SU},k}^{\mathrm{downlink}}$, is defined similarly. It can be seen from Fig. 5 that again the downlink per-user capacity for SUs achieved by our scheme is smaller compared with that of the conventional scheme, whereas both schemes achieve similar downlink per-user capacities for MUs. Considering the fact that our scheme can support more MUs, which inevitably leads to a significant increase of leakage in the precoding process, it is remarkable that it is capable of attaining a similar per-user capacity for MUs as the conventional scheme does.

Finally, we compare the total capacity per cell achieved by the two schemes, where the uplink sum rate is defined as

$$C^{\mathrm{uplink}} = \sum_{k=1}^{K_m} C_{\mathrm{MU},k}^{\mathrm{uplink}} + \sum_{k=1}^{P} C_{\mathrm{SU},k}^{\mathrm{uplink}} \tag{18}$$

and the downlink sum rate C^{downlink} is defined similarly. From Fig. 6, we observe that our scheme provides significantly higher sum-rate capacities for both uplink and downlink, as compared with the

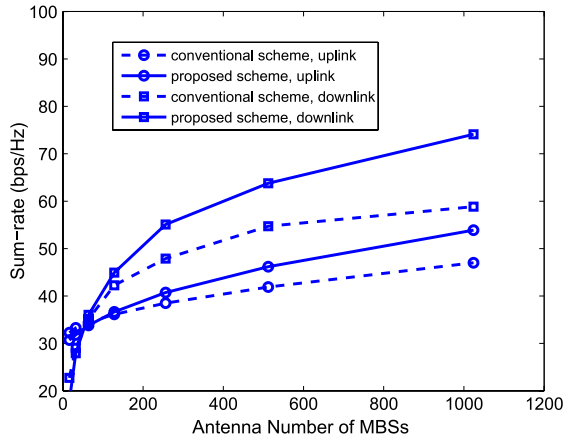

Fig. 6. Sum-rate comparison of both uplink data transmission with MF detection and downlink data transmission with ZF precoding.

conventional scheme. Additionally, the performance gain increases as the antenna number M increases. When M is equal to 1024, the uplink and downlink sum-rate capacities improve by 26% and 15%, respectively, as compared with the conventional scheme. These results thus demonstrate that our scheme can support more users and achieve a better performance for massive MIMO–HetNet systems.

V. Conclusion

We have proposed a pilot reuse scheme for massive MIMO–HetNet systems operating in coTDD mode, which employs the location-aware channel estimation for interference reduction. Our main novel contribution has been to propose a location-aware pilot assignment algorithm that is capable of reducing the interference in the system by ensuring that the users with the same pilot has different AOAs at MBSs, while the distance between the interfering users and the corresponding SBS is sufficiently large. Simulation results have demonstrated that our proposed scheme can support more users and increase the uplink and downlink sum-rate capacities, while only requiring very limited coordination between BSs.

References

[1] F. Rusek *et al.*, "Scaling up MIMO: Opportunities and challenges with very large arrays," *IEEE Signal Process. Mag.*, vol. 30, no. 1, pp. 40–60, Jan. 2013.

[2] L. Lu, G. Y. Li, A. L. Swindlehurst, A. Ashikhmin, and R. Zhang, "An overview of massive MIMO: Benefits and challenges," *IEEE J. Sel. Topics Signal Process.*, vol. 8, no. 5, pp. 742–758, Oct. 2014.

[3] H. Q. Ngo, E. G. Larsson, and T. L. Marzetta, "Energy and spectral efficiency of very large multiuser MIMO systems," *IEEE Trans. Commun.*, vol. 61, no. 4, pp. 1436–1449, Apr. 2013.

[4] J. G. Andrews, H. Claussen, M. Dohler, S. Rangan, and M. C. Reed, "Femtocells: Past, present, and future," *IEEE J. Sel. Areas Commun.*, vol. 30, no. 3, pp. 497–508, Apr. 2012.

[5] M. Kountouris and N. Pappas, "HetNets and massive MIMO: Modeling, potential gains, and performance analysis," in *Proc. IEEE-APS APWC*, Torino, Italy, Sep. 9–13, 2013, pp. 1319–1322.

[6] J. Hoydis, K. Hosseini, S. ten Brink, and M. Debbah, "Making smart use of excess antennas: Massive MIMO, small cells, and TDD," *Bell Labs Tech. J.*, vol. 18, no. 2, pp. 5–21, Sep. 2013.

[7] A. Hu, T. Lv, H. Gao, Y. Lu, and E. Liu, "Pilot design for large-scale multi-cell multiuser MIMO systems," in *Proc. IEEE ICC*, Budapest, Hungary, Jun. 9–13, 2013, pp. 5381–5385.

[8] M. Peng, X. Zhang, and W. Wang, "Performance of orthogonal and co-channel resource assignments for femto-cells in long term evolution systems," *IET Commun.*, vol. 5, no. 7, pp. 996–1005, May 2011.

[9] J. Zhang *et al.*, "Pilot contamination elimination for large-scale multiple-antenna aided OFDM systems," *IEEE J. Sel. Topics Signal Process.*, vol. 8, no. 5, pp. 759–772, Oct. 2014.
[10] Z. Wang *et al.*, "Location-based channel estimation and pilot assignment for massive MIMO systems," in *Proc. IEEE ICCW*, London, U.K., Jun. 8–12, 2015, pp. 1–5.
[11] Z. Zhao, Z. Chen, and Y. Liu, "Cell sectorization-based pilot assignment scheme in massive MIMO systems," in *Proc. WTS*, New York, NY, USA, Apr. 15–17, 2015, pp. 1–5.
[12] Q. He, L. Xiao, X. Zhong, and S. Zhou, "Increasing the sum-throughput of cells with a sectorization method for massive MIMO," *IEEE Commun. Lett.*, vol. 18, no. 10, pp. 1827–1830, Oct. 2014.
[13] H. Yin, D. Gesbert, M. Filippou, and Y. Liu, "A coordinated approach to channel estimation in large-scale multiple-antenna systems," *IEEE J. Sel. Areas Commun.*, vol. 31, no. 2, pp. 264–273, Feb. 2013.

Adaptive Index Modulation for Parallel Gaussian Channels With Finite Alphabet Inputs

Jianping Zheng

***Abstract*—In this paper, we extend the concept of adaptive spatial modulation to the parallel Gaussian channel with finite alphabet input and propose a transmit scheme called adaptive index modulation (AIM). In the proposed scheme, the transmitter adaptively selects the index modulation pattern, consisting of the active channel subset and the associated signal constellations, according to the criterion of maximizing the minimum squared Euclidean distance. To reduce the complexity, first, the number of candidate patterns in the selection procedure is reduced by employing the relation of the normalized signal constellations with different modulation orders. Second, a simple lookup table method is presented. Finally, the performance of the proposed scheme is demonstrated in both the scenarios of multicarrier transmission and multiantenna transmission by computer simulations.**

***Index Terms*—Adaptive modulation, finite alphabet input, index modulation (IM), parallel channel, spatial modulation (SM).**

I. Introduction

A parallel Gaussian channel is an important channel model in both the wireline and the wireless domains. For example, it can model the multitone transmission [1] and the singular-value decomposition (SVD)-based multiantenna communication [2]. Usually, the power allocation strategy is designed to maximize the mutual information of this channel. Under an average power constraint, it is well known that the strategy to allocate power according to the water-filling policy is optimal when the inputs to the channels are mutually independent as well as Gaussian [3]. However, the water-filling policy usually shows poor performance when finite alphabet inputs, i.e., signals from discrete signal constellation, are considered. In [4], the optimal power allocation with arbitrary input distributions is designed through utilizing the relation of mutual information and minimum mean square error (MMSE) [5]. In addition, the proposed mercury/water-filling (M/W) algorithm in [4] can find out the optimal power allocation using an iterative method, once the MMSE presentation with the receive signal-to-noise ratio (SNR) as the argument can be predetermined for arbitrary signal constellation.

Spatial modulation (SM) is a novel spatial multiplexing scheme proposed recently for multiple-input–multiple-output (MIMO) systems [6]–[11]. In SM, a new dimension, which is called spatial dimension, is introduced to convey information, which usually results in higher energy efficiency (EE) than conventional multiantenna schemes. Due to the high EE potential, SM has recently been researched extensively (for a recent survey, see [12] and [13]). Among those developments listed in [12] and [13], the adaptive SM [14], [15] attracts much interest since it can improve the error performance when partial or full channel state information (CSI) is known at the transmitter. In [14], an adaptive power-allocation algorithm is proposed to improve the error performance for the two-antenna space-shift keying scheme. In [15], a link-adaptive SM scheme is proposed where the signal constellation associated with each transmit antenna is selected adaptively according to the CSI. In [16], the adaptive SM is further extended to the case that both signal constellation associated with each transmit antenna and the number of active antennas can be varied adaptively. On the other hand, an important tendency of the SM research is the application scenario shifting from multiantenna systems to others. For example, in [17]–[19], the concept of SM is applied in the orthogonal frequency-division multiplexing (OFDM) system, where the proposed schemes are termed subcarrier index modulation (IM) in [17] and [18], as well as OFDM-IM in [19].

In this paper, we extend the concept of adaptive SM to the parallel Gaussian channel with finite alphabet input and propose a scheme called adaptive IM (AIM). Different from [4], the aim is minimizing the symbol error rate (SER) in the proposed scheme while maximizing the mutual information in the M/W method [4]. Moreover, the active channel subset and the associated signal constellations are adjusted in AIM, whereas the transmit power of each channel is adjusted in the M/W method. On the other hand, the proposed AIM can be viewed as an adaptive implementation of OFDM-IM when applied in the OFDM-based multicarrier transmission.

In the proposed AIM scheme, the IM pattern, consisting of the active channel subset and the associated signal constellations, is adaptively selected according to the channel strength to maximize the minimum squared Euclidean distance (ED). Utilizing the relation of normalized signal constellations with different modulation orders, the number of candidate patterns in the selection procedure can be reduced enormously. Furthermore, the adaptive pattern selection can be implemented by the lookup table method. Finally, the performance of the AIM is demonstrated by simulations, where the application scenarios of both the OFDM-based multicarrier transmission and the SVD-based multimultiple transmission are considered.

The main contribution of this paper is twofold. First, the concept of SM is extended from the multiantenna system to the parallel Gaussian channel with finite alphabet input. In addition, the resulted novel AIM scheme adjusts the number of active parallel channel subset and the signal constellation for each channel adaptively. This differs from the conventional power-allocation method [3], [4]. Second, the low-complexity implementation of AIM through candidate pattern reduction and lookup table method is given.

Manuscript received December 9, 2014; revised July 3, 2015; accepted September 2, 2015. Date of publication September 7, 2015; date of current version August 11, 2016. This work was supported in part by the China 973 Program under Grant 2012CB316100 and in part by the National Natural Science Foundation of China under Grant 61201140 and Grant 61372074. The review of this paper was coordinated by Dr. S. K. Jayaweera.

The author is with the State Key Laboratory of Integrated Services Networks, Xidian University, Xi'an 710071, China (e-mail: jpzheng@xidian.edu.cn).

Color versions of one or more of the figures in this paper are available online at http://ieeexplore.ieee.org.

Digital Object Identifier 10.1109/TVT.2015.2477078

0018-9545 © 2015 IEEE. Personal use is permitted, but republication/redistribution requires IEEE permission.
See http://www.ieee.org/publications_standards/publications/rights/index.html for more information.